

# Reconfigurable Transient Polymer Networks Based on Heteroleptic Metal–Ligand Complexes

Mostafa Ahmadi,\* Yasothaa Thavayogarajah, Josep Duran, Albert Poater, and Sebastian Seiffert

Cite This: *ACS Appl. Polym. Mater.* 2025, 7, 16427–16433

Read Online

ACCESS |



Metrics &amp; More



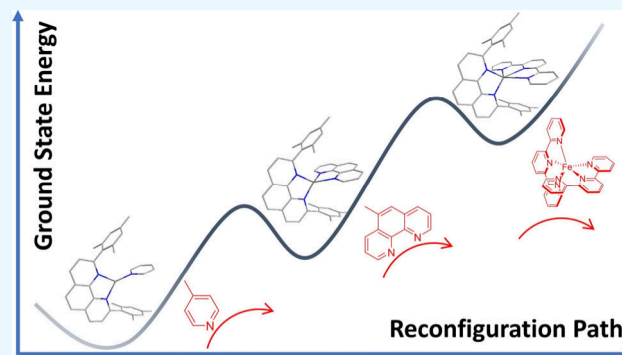
Article Recommendations



Supporting Information

**ABSTRACT:** We present a polymer network platform based on metal–ligand complexes that enables reconfiguration through the sequential introduction of polymeric ligands and metal ions. Using tetraPEG functionalized with sterically demanding and slim ligands, we demonstrate four network states. However, the interference from competitive parallel complexations is reflected in rheology as additional relaxation modes. A simple kinetic model rationalizes the extent of reconfiguration as a function of thermodynamic preference, revealing the critical role of competitive complexation. DFT calculations confirm that ligand denticity stabilizes heteroleptic complexes and drives the reconfiguration pathway. Together, experiment, modeling, and computation establish a comprehensive framework for designing reconfigurable transient polymer networks.

**KEYWORDS:** Supramolecular Polymers, Transient Networks, Reconfiguration, Metal Complex, Rheology



Nature has long served as a blueprint for the design of advanced functional materials. In biological systems, dynamic and reversible interactions play a central role in structural organization, mechanical adaptability, and complex signal transmission.<sup>1</sup> These interactions enable proteins to fold, cells to self-heal, and molecular machines like motor proteins to perform directional tasks reversibly and repeatedly.<sup>2</sup> For example, the reversible coordination between metal ions and amino acid residues is crucial in metalloproteins,<sup>3</sup> while hydrogen bonding and  $\pi$ – $\pi$  stacking govern DNA base pairing.<sup>4</sup> These mechanisms offer inspiration for chemists seeking to engineer responsive and reconfigurable synthetic systems.<sup>5</sup> Driven by this vision, researchers have increasingly focused on exploring novel supramolecular material platforms capable of capturing the same degree of structural complexity and functional versatility found in nature.

Among supramolecular interactions, metal–ligand coordination stands out for its modularity and geometric control, enabling the construction of well-defined architectures with predictable shapes.<sup>1,6,7</sup> Furthermore, recent self-sorting mechanisms have enabled selecting complexation of alike ligands (homoleptic) or unlike ones (heteroleptic).<sup>8,9</sup> One such mechanism is steric hindrance, which avoids the homoleptic complexation of sterically demanding ligands yet allows their heteroleptic binding with slim ones. Accordingly, by substituting phenanthroline<sup>9,10</sup> and terpyridine<sup>11,12</sup> with bulky aromatic groups on the coordination face, a wide library of complex yet predictable assemblies have been created. The reversible shifting between homo- and heteroleptic complexes enables sophisticated motions like shuttling, pirouetting, and

flapping in interlocked molecules like rotaxanes and catenanes, which has been exploited to develop a range of molecular machines.<sup>9,13</sup> Notably, the first artificial molecular muscle was developed by integrating bi- and tridentate ligands in a daisy chain.<sup>14</sup> Switching of the metal oxidation state changed the preferred binding station, swapping between homo- and heteroleptic complexation, which resulted in deformation at the molecular scale.

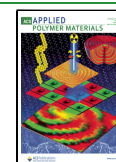
Beyond small-molecule systems, homo- and heteroleptic complexes have been incorporated in transient polymer networks, enabling model networks with predictable architectures, stimuli-responsiveness, and self-healing behavior.<sup>15–19</sup> However, reconfiguration strategies have been typically limited to variation of the coordination geometry via redox switching or the addition of competitive small-molecule ligands.<sup>20–22</sup> The sophisticated reconfiguration developed in molecular machines, like the multistep pathway-controlled rearrangements between distinct geometries,<sup>9</sup> has not been employed in polymeric systems.<sup>23</sup> Specifically, the reversible interconversion between homo- and heteroleptic complexes as a means of network reconfiguration remains unexplored. Harnessing such mechanisms could yield macromolecular machines with

Received: September 12, 2025

Revised: December 8, 2025

Accepted: December 8, 2025

Published: December 11, 2025



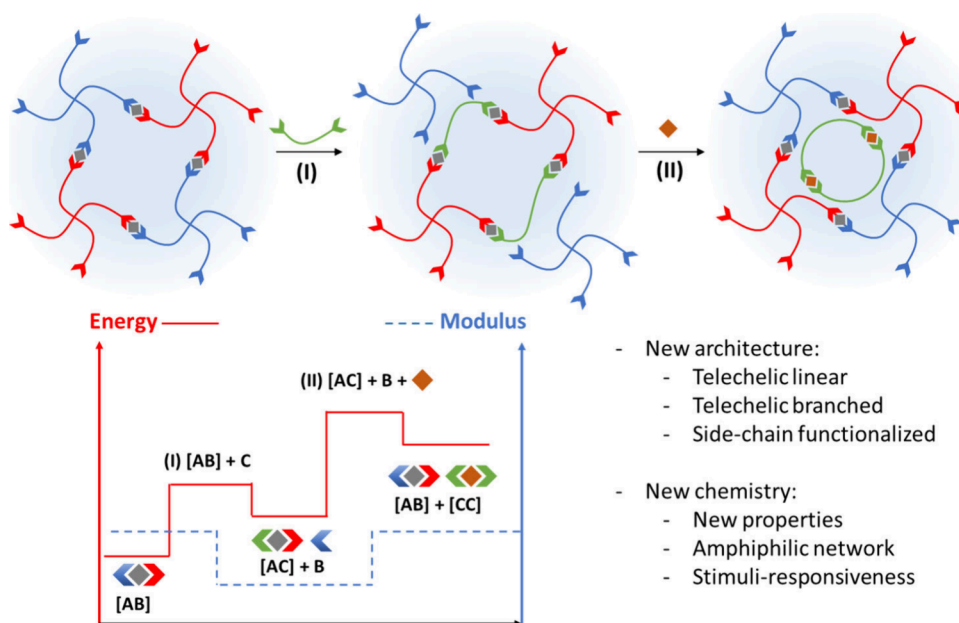


**Figure 1.** Schematic of the ideal reversible network reconfiguration and expected evolution of network energy and modulus. (I) The added green polymer segment forms stronger complexes. (II) The original network is restored upon introducing a new metal ion that forms stronger complexes with the green segment. Reconfiguration enables changing the network properties by introducing segments with new architectures and chemistries.

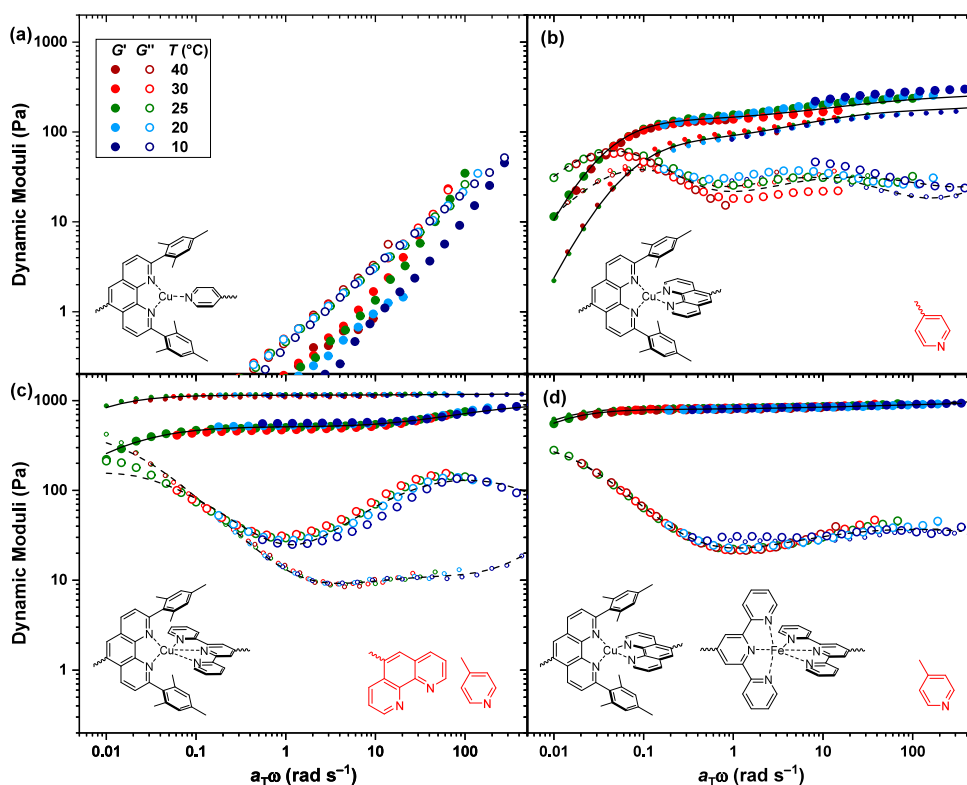


**Figure 2.** Dynamic moduli master curves (symbols) of  $\text{Cu}^{2+}$  networks: (a) Network (I) formed by tetraDMPhen20k and tetraPy20k; (b) Network (II) formed by introducing LPhen3k and the release of tetraPy20k; (c) Network (III) formed by introducing tetraTPy20k and the further release of LPhen3k; and (d) Network (IV) formed by the addition of  $\text{Fe}^{2+}$ , restoring the DMPHEN–Phen complex with  $\text{Cu}^{2+}$  and the new bis TPY– $\text{Fe}^{2+}$  complex. Dots show the dynamic moduli master curves of the corresponding control networks formed in the absence of the expected free precursors highlighted in red. The temperature legend shown in (a) is valid for all panels. Lines show the fit of the generalized Maxwell model.

temporally programmed behavior and multiple structural states.

One potential strategy to enable reconfigurable metallo-supramolecular polymer networks would be to introduce a new

polymer segment bearing a competitive ligand that increases the overall energy but establishes a new thermodynamic equilibrium with a higher binding affinity (Figure 1). If the new segment shares the parent architecture, the mechanics

remain unchanged, while the network lifetime typically increases. Using different architectures or chemistries alters the topology or introduces new properties such as amphiphilicity or thermo-responsiveness. Reconfiguration can be reversed by adding a metal ion with stronger affinity for the new ligand, restoring the original network with the weaker complex. Depending on the architecture of the added polymer segment, the complex with the higher binding affinity could form a second, interpenetrating network or form extended soluble chains and loops, with less effect on the mechanics. This ideal image requires sequential and clean substitution of precursors and metal complexes. However, the risk of competitive complexation can limit the extent of reconfiguration.

As a proof of concept, herein we introduce a transient polymer network platform, which allows three steps of reconfiguration by introducing either new polymeric ligands or new metal ions. Specifically, we functionalized a  $20 \text{ kg mol}^{-1}$  tetra-arm poly(ethylene glycol) (tetraPEG20k) either with the sterically demanding 2,9-bis(mesitylene)-1,10-phenanthroline (DMPhen) ligand (tetraDMPhen20k) or with the slim pyridine (Py) ligand (tetraPy20k) (details of the synthesis and characterization are given in the Supporting Information (SI), Figures S1–S5).<sup>18</sup> We formed Network (I) by mixing polymer precursors in a 1:1 ratio, right at the coil overlap concentration of  $40 \text{ g L}^{-1}$  in the presence of  $\text{Cu}^{2+}$  metal ions.<sup>24</sup> This heteroleptic complex, already named HETPYP,<sup>9</sup> is reported to have a high dissociation rate constant, resulting in dissolution of the network at short times. The small-amplitude oscillatory shear (SAOS) measurement shows that the crossover of the storage and loss moduli, which is a measure of the gel–sol transition, is located at frequencies above the experimentally accessible regime (Figure 2a). The heteroleptic arrangement of ligands dictates a trigonal geometry; therefore, the coordination preference of  $\text{Cu}^{2+}$  is presumably compensated by the coordination of solvent or counterions.

Stronger complexes are expected to form upon increasing the number of coordinative bonds,<sup>16</sup> for instance, by replacing Py with the bidentate phenanthroline (Phen). As such, introducing a different polymer precursor equipped with Phen should reconfigure the network structure and dynamics and release the tetraPy20k precursor. To verify that, we added a  $3 \text{ kg mol}^{-1}$  linear PEG precursor functionalized with terminal Phen groups (LPhen3k) at an equimolar ratio of DMPhen:Phen to Network (I). Replacing the tetraPy20k with a short linear precursor should significantly change the network mechanics along with the dynamics. The dynamic moduli master curve of the reconfigured Network (II) indicates the presence of at least two relaxation modes, as comprehended from local peaks in the loss modulus at  $\sim 0.03$  and  $\sim 10 \text{ rad s}^{-1}$ . The newly appearing slow relaxation mode can be attributed to the dissociation of tetrahedral HETPHEN complexes. We fit the dynamic moduli with the weighted summation of two generalized Maxwell modes, each represented by a Gaussian distribution function, to separate the contribution of each relaxation mode (Table S1). The obtained relaxation times of the slow modes that are located below the accessible frequency range are just rough estimates, although their intensities are reliable. The obtained relaxation time spectrum (Figure S6) reveals a bimodal relaxation with an  $\sim 42\%$  contribution of the slow mode. The control sample prepared by mixing tetraDMPhen20k and LPhen3k, in the absence of the

expectedly free tetraPy20k (dots in Figure 2), demonstrates a two-mode relaxation pattern with time scales similar to those of Network (II), with slightly different fractions and less time–temperature complexity. The fast mode could be associated with the parallel formation of competitive complexes. This includes not only the homoleptic complexation of released tetraPy20k precursors but also the residual fraction of the heteroleptic DMPhen–Py complex and consequent homoleptic complexation of extra Phen ligands. The formation of parallel networks reduces the amount of metal ion available for the desired reconfiguration, resulting in plateau moduli that are less than the prediction of the phantom network model (Table S1).

As  $\text{Cu}^{2+}$  is known for its penta-coordinated geometry preference,<sup>16</sup> next we introduced a tetraPEG20k precursor equipped with terminal tridentate terpyridine (TPy) ligands (tetraTPy20k) at an equimolar ratio of DMPhen:TPy to Network (II). Returning the tetrafunctional precursor is expected to restore the network mechanics and change the dynamics accordingly. The dynamic moduli of Network (III) demonstrate a similar two-mode relaxation (Figure 2c). However, the plateau modulus is tripled, the contribution of the slow mode is increased from  $\sim 42\%$  to  $\sim 55\%$ , and the relaxation time of the slow mode is increased from 24 to 102 s (Table S2). The control network formed by a 1:1 combination of tetraDMPhen20k:tetraTPy20k at an overall concentration of  $40 \text{ g L}^{-1}$ , in the absence of the additional LPhen3k and tetraPy20k, demonstrates a similar bimodal relaxation but with  $\sim 94\%$  contribution of the slow mode and a larger plateau modulus, as shown by dots. Therefore, the slow mode in the reconfigured Network (III) can be associated with the HETTAP complexes formed between DMPhen and TPy. Interestingly, the control network in Figure 2b shows a lower plateau modulus than Network (II), but the opposite trend appears in Figure 2c. This arises because the control network of tetraDMPhen20k–LPhen3k lies well below the chain overlap concentration; thus, the extra tetraPy20k in Network (II) can bridge chains and increase the modulus. In contrast, the tetraDMPhen20k–tetraTPy20k control network is on the overlap concentration, so the extra tetraPy20k and LPhen3k in Network (III) form parallel networks that deplete the metal ions needed for reconfiguration, thereby reducing the modulus.

A quite unique nanomechanical motion was devised in a macrocycle containing two Phen and two TPy ligands placed in alternating order.<sup>25</sup> While Phen ligands form a tetrahedral complex in the presence of  $\text{Cu}^+$ , the addition of  $\text{Fe}^{2+}$  dictates the formation of the octahedral bis TPy complex, thus switching the topology of the macrocycle from the figure eight to  $\infty$ . The preference of octahedral over penta-coordinated complexation in nanoswitches containing DMPhen and TPy was similarly exploited.<sup>26</sup> Accordingly, adding  $\text{Fe}^{2+}$  to Network (III) should restore Network (II), along with an interpenetrating network formed between tetraTPy20k and  $\text{Fe}^{2+}$ . The corresponding dynamic moduli of Network (IV) (Figure 2d) demonstrate increased terminal relaxation time and plateau modulus. Moreover, the contribution of the slow mode is increased to  $\sim 80\%$  (Table S1). The individual tetraTPy20k network formed with  $\text{Fe}^{2+}$  at a concentration of  $20 \text{ g L}^{-1}$  (half of the overlap concentration) demonstrates an order of magnitude lower plateau modulus and a more than 2 orders of magnitude larger relaxation time (Figure S7). Therefore, the third mode relaxation of bis TPy– $\text{Fe}^{2+}$  complexes in Network (IV) cannot be accessed in the

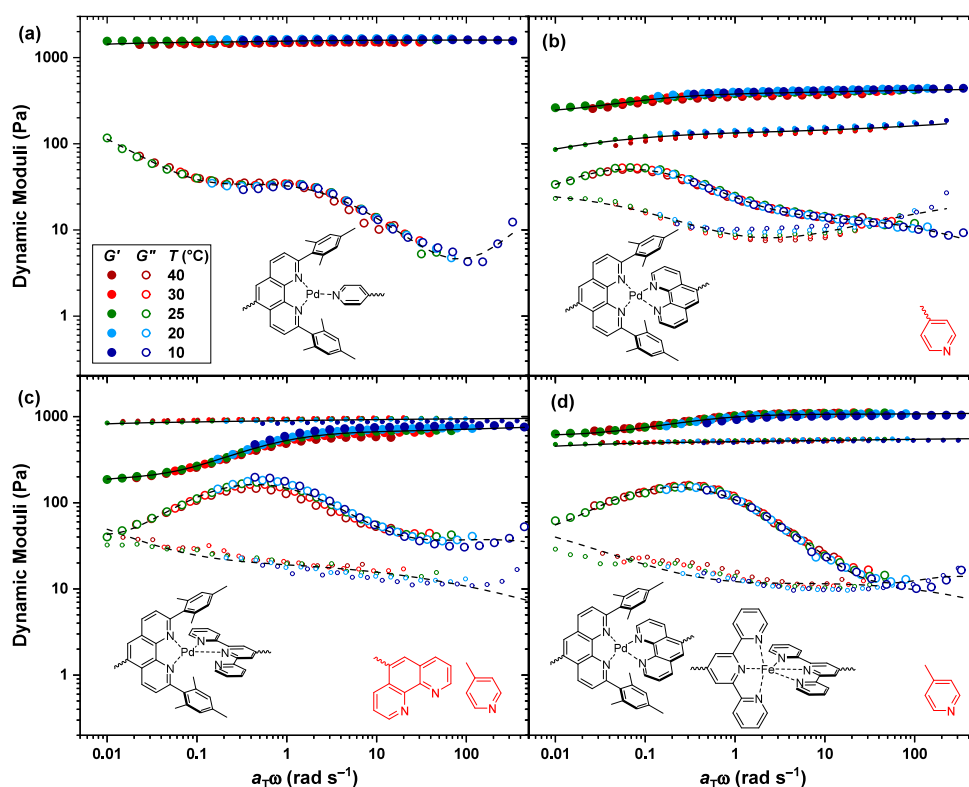


**Figure 3.** Dynamic moduli master curves (symbols) of Pd<sup>2+</sup> networks: (a) Network (I) formed by tetraDMPPhen20k and tetraPy20k; (b) Network (II) formed by introducing LPhen3k; (c) Network (III) formed by introducing tetraTPy20k; and (d) Network (IV) formed by the addition of Fe<sup>2+</sup>. Dots show the dynamic moduli master curves of the corresponding control networks formed in the absence of the expected free precursors highlighted in red. The temperature legend shown in (a) is valid for all panels. Lines show the fit of the generalized Maxwell model.

low-frequency region. Interestingly, there is no sign of the fast HETPHEN complex (compared to Network (II) in Figure 2b). We can hypothesize that the presence of the interpenetrated tetraTPy20k network has resulted in an order of magnitude delay in the apparent relaxation time of the HETPHEN complexes. Remarkably, the control sample formed in the absence of the tetraPy20k precursor, shown by dots, reveals exactly the same plateau modulus and crossover frequency as those of Network (IV).

The extent of reconfiguration relies on microscopic complex selectivity, which depends not only on the ligand design but also on the coordination geometry preference of the employed metal ion.<sup>16,17</sup> To verify that, we formed the same set of samples with Pd<sup>2+</sup> to study the effect of the square-planar geometry preference of Pd<sup>2+</sup> over the penta-coordination affinity of Cu<sup>2+</sup>. The obtained dynamic moduli master curves of the Pd<sup>2+</sup> networks (Figure 3) similarly demonstrate two-mode relaxation patterns (relaxation time spectra in Figure S8). The variations in the network mechanics and dynamics upon reconfiguration are also similar to the trends seen in the Cu<sup>2+</sup> networks. Specifically, upon replacing the tetraPy20k with the LPhen3k precursor, the plateau modulus drops significantly, but it is gradually restored upon the addition of tetraTPy20k and Fe<sup>2+</sup> metal ions (Table S2). The relaxation time of the slow mode is always below the accessible frequency range, but its contribution can be calculated from the low-frequency plateau modulus level, changing from  $\sim 92$  to  $\sim 50$ ,  $\sim 22$ , and  $\sim 54$  from Network (I) to Network (IV), respectively. Accordingly, the network reconfiguration can be confirmed from the change in network mechanics. Consequently, the coordination geometry preference has a direct

effect on the reconfiguration extent. For instance, Pd<sup>2+</sup> (square-planar) shows less compatibility to HETTAP compared to Cu<sup>2+</sup> (trigonal bipyramidal), and therefore, Network (III) forms less effectively in the presence of Pd<sup>2+</sup>.

We also employed unsubstituted Phen instead of the sterically demanding DMPPhen in the presence of Pd<sup>2+</sup>. This way we can verify the effect of the enforced versus free formation of heteroleptic complexes. In the absence of steric hindrance, the extent of heteroleptic complexation depends only on the coordination geometry preference of the metal ion.<sup>18,27</sup> This is clearly reflected in dynamic moduli and relaxation time spectra of networks formed upon replacing tetraDMPPhen20k with tetraPhen20k (Figures S9 and S10). When new polymer precursors are introduced, the competition of homo- and heteroleptic complexes, in the absence of enough metal ions, results in the formation of complexed branched chains instead of a percolated network. As such, while Network (I) demonstrates a plateau modulus close to the expectations of the phantom network model, Network (II) shows a one order of magnitude lower plateau modulus, and Network (III) does not form at all (Table S3). Network (IV) demonstrates a low-frequency plateau level that is expected from individual tetraTPy20k precursors in combination with Fe<sup>2+</sup> (compare Figures S7 and S9d).

Our rough estimates of the radius of gyration of PEG precursors from their chain overlap concentrations and the network mesh size based on the measured plateau moduli (Section S3 in the SI) suggest that in the worst scenario, the newly introduced precursor is about five times smaller than the network mesh size; therefore, there is no physical obstacle for the diffusion of the new precursors. Diffusion time scales with

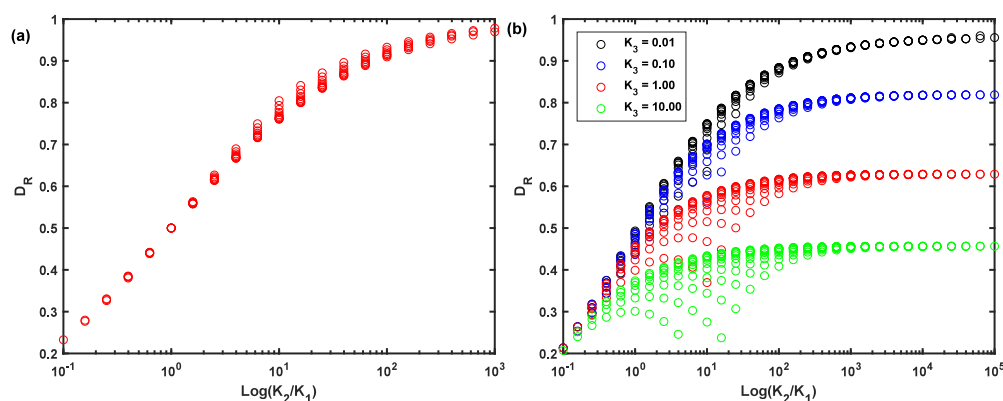


**Figure 4.** Reconfiguration degree as a function of the relative strength of the new complex ( $K_2/K_1$ ) for a kinetic scheme (a) without and (b) with the chance of homoleptic complexation of the leaving group, as explained by the corresponding  $K_3$  values (formation of homoleptic octahedral complexes,  $L^5 \text{ mol}^{-5}$ ) shown in the legend.

the lifetime of transient bonds following the sticky Rouse relaxation mechanism, as explained elsewhere.<sup>28</sup>

Consequently, reconfiguration of transient networks requires three important conditions. (1) The difference between energy levels of State (I) and State (II) should be large enough to avoid the parallel existence of State (I); otherwise, reconfiguration may happen, but only partially. (2) If the released polymer precursor can form independent bonds, a parallel network forms at the expense of reconfiguration. This is specifically relevant in metallo-supramolecular networks, as homoleptic complexes consume metal ions required for establishing the desired heteroleptic complexes. (3) The polymer precursor that stays in the active network in all reconfiguration states should exclusively form heterocomplementary bonds. This is easy to implement in covalent adaptable networks (CANs),<sup>29</sup> as cross-links typically form between complementary functional groups, like acids and bases; however, in metallo-supramolecular complexes, specific ligands should be devised to dictate the integrative self-sorting mechanism.<sup>6,8,30</sup>

To verify these conditions, we developed a simple thermodynamic model, where we can test the degree of reconfiguration as a function of the thermodynamic equilibrium. In this model, the incoming group C can establish a new product, AC, which requires reversing the product AB and leaving B unreacted (Kinetic Scheme S1 in the SI). The degree of reconfiguration,  $D_R$ , is defined as the fraction of [AC] in the product ( $[AB] + [AC]$ ). If we consider equimolar feed ratios,  $[A]_0 = [B]_0 = [C]_0$ , then  $D_R$  can be obtained as a function of equilibrium constants of the first and second states ( $K_1$  and  $K_2$ ) (Figure S11). All curves would lay on top of each other and form a matrix curve if  $D_R$  is plotted against the ratio of  $K_2/K_1$  (Figure 4a). Accordingly, regardless of the absolute values of the equilibrium constants, 50% reconfiguration is obtained at  $K_2/K_1 = 1$ , which is increased to 75% just by employing  $K_2/K_1 = 10$ . Reconfiguration becomes more complicated when leaving group B would form homoleptic complexes, as defined by the third equilibrium ( $K_3$ ) (Kinetic Scheme S2 in the SI). While all curves collapse on a single master curve at low  $K_3$  values, as  $K_3$  increases,  $D_R$  decreases, and curves obtained at lower  $K_1$  values deviate toward lower  $D_R$  numbers (Figures 4b and S12). Accordingly, even with a slight tendency for homoleptic complexation, regardless of the strength of the new complex ( $K_2/K_1$  value),  $D_R$  may decrease significantly.

To obtain an estimate of the energy levels of different reconfiguration states in our work, we used DFT calculations.

The results (Tables S4 and S5; finished with “q” meaning quintuplet multiplicity for  $\text{Fe}^{2+}$ , for  $\text{Pd}^{2+}$  always singlet), are not surprising. The energy levels of all heteroleptic complexes decrease by increasing the denticity of the slim ligand as we go from Py to Phn and TPy, enabling the reconfiguration in the presence of both  $\text{Pd}^{2+}$  and  $\text{Cu}^{2+}$ . Interestingly, the homoleptic association of  $\text{Fe}^{2+}$  with TPy is more stable than the corresponding HETPYP and HETPHEN complexes; however, HETTAP is more stable by just 2.3 kcal mol<sup>-1</sup>, which is in the order of calculation error. In comparison, homoleptic complexation with three Phn ligands is disfavored. The most quantitative summary is that the ligand denticity increases the binding affinity of heteroleptic complexes.

In conclusion, we demonstrated that the inevitable parallel formation of competitive reversible bonds can limit the overall degree of reconfiguration in systems based on reversible interactions. This challenge is clear in metallo-supramolecular polymer networks because of (I) the competition of the old and new heteroleptic complexes, (II) the homoleptic complexation of the replaced ligand, and (III) the possible homoleptic association of sterically demanding ligands. Nevertheless, we showed that the extent of reconfiguration can be optimized by selecting metal ions and heteroleptic complexes with compatible geometries. We indicated that the combination of rheology, kinetic modeling, and DFT calculations gives a useful guideline for designing polymer networks with tunable properties and even the potential to act as macromolecular machines in the future. Altogether, this study highlights both the opportunities and the limitations of reversible interactions for building multistep adaptive materials.

## ASSOCIATED CONTENT

### Supporting Information

The Supporting Information is available free of charge at <https://pubs.acs.org/doi/10.1021/acsapm.5c03436>.

Details of synthesis and characterization, additional SAOS data, calculated relaxation time spectra, fit parameters of the generalized Maxwell model and expected moduli of the phantom and affine network models, kinetic schemes, and ground state energies of all complexes as calculated by DFT and their XYZ coordinates (PDF)

## AUTHOR INFORMATION

### Corresponding Author

**Mostafa Ahmadi** – Department of Chemistry, Johannes Gutenberg-Universität Mainz, D-55128 Mainz, Germany; [orcid.org/0000-0001-6652-4067](https://orcid.org/0000-0001-6652-4067); Email: [ahmadi@uni-mainz.de](mailto:ahmadi@uni-mainz.de)

### Authors

**Yasothaa Thavayogarahaj** – Department of Chemistry, Johannes Gutenberg-Universität Mainz, D-55128 Mainz, Germany

**Josep Duran** – Institut de Química Computacional i Catàlisi, Departament de Química, Universitat de Girona, 17003 Girona, Catalonia, Spain; [orcid.org/0000-0003-2121-6364](https://orcid.org/0000-0003-2121-6364)

**Albert Poater** – Institut de Química Computacional i Catàlisi, Departament de Química, Universitat de Girona, 17003 Girona, Catalonia, Spain; [orcid.org/0000-0002-8997-2599](https://orcid.org/0000-0002-8997-2599)

**Sebastian Seiffert** – Department of Chemistry, Johannes Gutenberg-Universität Mainz, D-55128 Mainz, Germany; [orcid.org/0000-0002-5152-1207](https://orcid.org/0000-0002-5152-1207)

Complete contact information is available at: <https://pubs.acs.org/10.1021/acsapm.5c03436>

### Notes

The authors declare no competing financial interest.

## ACKNOWLEDGMENTS

Funding from the DFG (Deutsche Forschungsgemeinschaft) is acknowledged: SFB 1552 (project No. 465145163) [M.A., Y.T.], individual research grant (project No. 491930291) [M.A.]. A.P. is a Serra Hünter Fellow and thanks the Spanish MINECO for project PID2024-155989NB-I00 and the Generalitat de Catalunya for project 2021SGR623.

## REFERENCES

- (1) Khare, E.; Holtén-Andersen, N.; Buehler, M. J. Transition-metal coordinate bonds for bioinspired macromolecules with tunable mechanical properties. *Nat. Rev. Mater.* **2021**, *6* (5), 421–436.
- (2) Kolomeisky, A. B. Motor proteins and molecular motors: how to operate machines at the nanoscale. *J. Phys.: Condens. Matter* **2013**, *25* (46), No. 463101.
- (3) Yang, M.; Song, W. J. Diverse protein assembly driven by metal and chelating amino acids with selectivity and tunability. *Nat. Commun.* **2019**, *10* (1), 5545.
- (4) Ohira, M.; Katashima, T.; Naito, M.; Aoki, D.; Yoshikawa, Y.; Iwase, H.; Takata, S. i.; Miyata, K.; Chung, U. i.; Sakai, T.; et al. Star-Polymer–DNA Gels Showing Highly Predictable and Tunable Mechanical Responses. *Adv. Mater.* **2022**, *34* (13), No. 2108818.
- (5) Lehn, J. M. Perspectives in chemistry—steps towards complex matter. *Angew. Chem., Int. Ed.* **2013**, *52* (10), 2836–2850.
- (6) Hosseinzadeh, B.; Ahmadi, M. Coordination geometry in metallo-supramolecular polymer networks. *Coord. Chem. Rev.* **2022**, *471*, No. 214733.
- (7) Smulders, M. M.; Riddell, I. A.; Browne, C.; Nitschke, J. R. Building on architectural principles for three-dimensional metallo-supramolecular construction. *Chem. Soc. Rev.* **2013**, *42* (4), 1728–1754.
- (8) Lewis, J. E. M.; Crowley, J. D. Metallo-Supramolecular Self-Assembly with Reduced-Symmetry Ligands. *ChemPlusChem.* **2020**, *85* (5), 815–827.
- (9) Goswami, A.; Saha, S.; Biswas, P. K.; Schmittel, M. (Nano)-mechanical Motion Triggered by Metal Coordination: from Functional Devices to Networked Multicomponent Catalytic Machinery. *Chem. Rev.* **2020**, *120* (1), 125–199.
- (10) Schmittel, M.; Michel, C.; Liu, S. X.; Schildbach, D.; Fenske, D. New Sterically Encumbered 2, 9-Diarylphenanthrolines for the Selective Formation of Heteroleptic Bis (phenanthroline) copper (I) Complexes. *Eur. J. Inorg. Chem.* **2001**, *2001* (5), 1155–1166.
- (11) He, Y.-J.; Tu, T.-H.; Su, M.-K.; Yang, C.-W.; Kong, K. V.; Chan, Y.-T. Facile construction of metallo-supramolecular poly (3-hexylthiophene)-block-poly (ethylene oxide) diblock copolymers via complementary coordination and their self-assembled nanostructures. *J. Am. Chem. Soc.* **2017**, *139* (11), 4218–4224.
- (12) Tu, T. H.; Sakurai, T.; Seki, S.; Ishida, Y.; Chan, Y. T. Towards Macroscopically Anisotropic Functionality: Oriented Metallo-supramolecular Polymeric Materials Induced by Magnetic Fields. *Angew. Chem., Int. Ed. Engl.* **2021**, *60* (4), 1923–1928.
- (13) Ghiassinejad, S.; Ahmadi, M.; Van Ruymbeke, E.; Fustin, C.-A. Dynamics of ring-containing polymers: Macromolecular rotaxanes, polyrotaxanes and slide-ring networks. *Prog. Polym. Sci.* **2024**, *155*, No. 101854.
- (14) Sauvage, J. P. From chemical topology to molecular machines (Nobel lecture). *Angew. Chem., Int. Ed.* **2017**, *56* (37), 11080–11093.
- (15) Ahmadi, M.; Poater, A.; Seiffert, S. Self-Sorting of Transient Polymer Networks by the Selective Formation of Heteroleptic Metal-Ligand Complexes. *Macromolecules* **2023**, *56* (4), 1390–1401.
- (16) Ahmadi, M.; Poater, A.; Seiffert, S. Decoding Coordination Geometry Enforcement in Metallo-Supramolecular Polymer Networks from Macroscopic Rheological Signatures. *Macromolecules* **2024**, *57*, 8803–8812.
- (17) Ahmadi, M.; Seiffert, S. Coordination geometry preference regulates the structure and dynamics of metallo-supramolecular polymer networks. *Macromolecules* **2021**, *54* (3), 1388–1400.
- (18) Ahmadi, M.; Seiffert, S. Direct Evidence of Heteroleptic Complexation in the Macroscopic Dynamics of Metallo-supramolecular Polymer Networks. *Macromolecules* **2021**, *54* (15), 7113–7124.
- (19) Ahmadi, M.; Löser, L.; Pareras, G.; Poater, A.; Saalwächter, K.; Seiffert, S. Connectivity Defects in Metallo-Supramolecular Polymer Networks at Different Self-Sorting Regimes. *Chem. Mater.* **2023**, *35* (10), 4026–4037.
- (20) Harris, R. D.; Auletta, J. T.; Motlagh, S. A. M.; Lawless, M. J.; Perri, N. M.; Saxena, S.; Weiland, L. M.; Waldeck, D. H.; Clark, W. W.; Meyer, T. Y. Chemical and electrochemical manipulation of mechanical properties in stimuli-responsive copper-cross-linked hydrogels. *ACS Macro Lett.* **2013**, *2* (12), 1095–1099.
- (21) Holtén-Andersen, N.; Harrington, M. J.; Birkedal, H.; Lee, B. P.; Messersmith, P. B.; Lee, K. Y. C.; Waite, J. H. pH-induced metal-ligand cross-links inspired by mussel yield self-healing polymer networks with near-covalent elastic moduli. *Proc. Natl. Acad. Sci. U.S.A.* **2011**, *108* (7), 2651–2655.
- (22) Wegner, S. V.; Schenk, F. C.; Witzel, S.; Bialas, F.; Spatz, J. P. Cobalt cross-linked redox-responsive PEG hydrogels: From viscoelastic liquids to elastic solids. *Macromolecules* **2016**, *49* (11), 4229–4235.
- (23) Goujon, A.; Moulin, E.; Fuks, G.; Giuseppone, N. [c 2] Daisy chain rotaxanes as molecular muscles. *CCS Chemistry* **2019**, *1* (1), 83–96.
- (24) Schmolke, W.; Ahmadi, M.; Seiffert, S. Enhancement of metallo-supramolecular dissociation kinetics in telechelic terpyridine-capped poly(ethylene glycol) assemblies in the semi-dilute regime. *Phys. Chem. Chem. Phys.* **2019**, *21* (35), 19623–19638.
- (25) Niess, F.; Duplan, V.; Sauvage, J.-P. Interconversion between a vertically oriented transition metal-complexed figure-of-eight and a horizontally disposed one. *J. Am. Chem. Soc.* **2014**, *136* (16), 5876–5879.
- (26) Mittal, N.; Pramanik, S.; Paul, I.; De, S.; Schmittel, M. Networking nanoswitches for ON/OFF control of catalysis. *J. Am. Chem. Soc.* **2017**, *139* (12), 4270–4273.
- (27) Ahmadi, M.; Sprenger, C.; Pareras, G.; Poater, A.; Seiffert, S. Self-organization of metallo-supramolecular polymer networks by free

formation of pyridine-phenanthroline heteroleptic complexes. *Soft Matter* **2023**, *19* (42), 8112–8123.

(28) Ramirez, J.; Dursch, T. J.; Olsen, B. D. A molecular explanation for anomalous diffusion in supramolecular polymer networks. *Macromolecules* **2018**, *51* (7), 2517–2525.

(29) Jia, Y.; Qian, J.; Hao, S.; Zhang, S.; Wei, F.; Zheng, H.; Li, Y.; Song, J.; Zhao, Z. New Prospects Arising from Dynamically Crosslinked Polymers: Reprogramming Their Properties. *Adv. Mater.* **2024**, *36* (21), No. 2313164.

(30) Jin, T.; Zhang, X.; Su, J.-Y.; Ding, J.-X.; Dou, W.-T.; Xu, L. Exploring self-sorting in metallacycles: Toward advanced supramolecular systems and materials. *Supramolecular Materials* **2025**, *4*, No. 100117.